2021 NDIA GROUND VEHICLE SYSTEMS ENGINEERING AND TECHNOLOGY SYMPOSIUM
ADDITIVE MANUFACTURING TECHNICAL SESSION
AUGUST 10-12, 2021 - NOVI, MICHIGAN

Robotic GMA-P DED AM Build Technology for Aluminum Vehicle Structures

Canaday, J.,[1] Harwig, D.D.[1,2], and Carney, M.[2]
[1] The Ohio State University Columbus, OH
[2]EWI Columbus, OH

ABSTRACT

Gas metal arc pulse directed energy deposition (GMA-P DED) offers large-scale additive manufacturing (AM) capabilities and lower cost systems compared to laser or electron beam DED. These advantages position GMA-DED as a promising manufacturing process for widespread industrial adoption. To enable this "digital" manufacturing of a component from a computer-aided design (CAD) file, a computer-aided manufacturing (CAM) solver is necessary to generate build plans and utilize welding parameter sets based on feature and application requirements. Scalable and robot-agnostic computer-aided robotics (CAR) software is therefore essential to provide automated toolpath generation. This work establishes the use of Autodesk PowerMill Ultimate software as a CAM/CAR solution for arc-based DED processes across robot manufacturers. Preferred aluminum GMA-P DED welding parameters were developed for single-pass wide "walls" and multi-pass wide "blocks" that can be configured to build a wide range of features and components from ER5183. These parameters were incorporated into Autodesk PowerMill Ultimate to create several representative builds using GMA-DED of ER5183 with an 8-axis OTC Daihen GMA robot cell.

Citation: Canaday, J., Harwig, D.D., and Carney, M. "Robotic GMA-P DED AM Build Technology for Aluminum Vehicle Structures", In *Proceedings of the Ground Vehicle Systems Engineering and Technology Symposium* (GVSETS), NDIA, Novi, MI, Aug. 13-15, 2021.

1. INTRODUCTION

The multitude of advantages proposed by the adoption of additive manufacturing (AM) processes has sparked immense research and commercialization efforts across all sectors of manufacturing. These motivations suggest reduced costs and lead times while offering increased design freedoms (3,4). Additional applications of this technology enable the repair or replacement of components for legacy equipment with out-of-production parts (3). For the additive manufacturing of metallic parts, the two primary approaches per ASTM terminology are powder bed fusion (PBF) and directed energy deposition (DED) (4). PBF processes are generally limited to small scale, high detail components which benefit from the precision of the laser/electron beam heat source and controlled powder bed environment. This contrasts with DED processes which achieve much greater build volumes and high deposition

Approved for Public Release - Sponsored NSF I/U CRC Ma2jic - "Any opinions, findings, and conclusions or recommendations expressed in this material are those of the author and do not necessarily reflect the views of the Ma2jic or its sponsors

rates which reduced accuracy by applying laser, electron beam, or welding arc to melt wire or powder feedstocks. When comparing these melting techniques, arc-based DED has numerous advantages which position it as most suitable for widespread industrial adoption: the maturity of arc-based welding process can leverage the existing base of knowledge and significant standardization efforts in addition to offering greatly reduced machine and feedstock costs (3,4,8). Further, the widespread availability of industrial arc welding equipment indicates great potential for immediate incorporation by manufacturers and researchers to advance the body of knowledge on this process. This also contrasts with the heightened complexity, capital investment, and safety concerns associated with laser and electron beam power sources.

Following deposition, the as-deposited arc DED build surface typically requires a post-machining operation to obtain precise geometric tolerances, depending on application. Requirement of an additional machining step may place barriers on the hypothetical design freedom promised by metal AM as access to all regions to be machined may be difficult (3,4,12).

Digital manufacturing approaches incorporate numerous software tools for part design, prototyping, and production. Directed energy deposition has emerged as a natural step in this progression as it can be classified as a "digital" manufacturing process since software is involved throughout (3). Initially, a designed CAD file for a given component is imported into a slicing software which deconstructs the component into a series of paths making up each layer. Further post-processing adds the necessary toolpath motion and welding instructions needed to generate a desired part. When considering DED systems, most research currently applies a 3-axis build model using a CNC style test bed. Welding knowledge motivates the modification of welding torch angle and work angle to achieve higher quality deposits which requires use of higher-axis robotic platforms to surpass the limitations of a torch-normal CNC configuration (11). Further flexibility and process control is also enabled by higher axis build approaches which can incorporate build platform manipulation, a step beyond higher order robot control, to further improve productivity and welding capability (12).

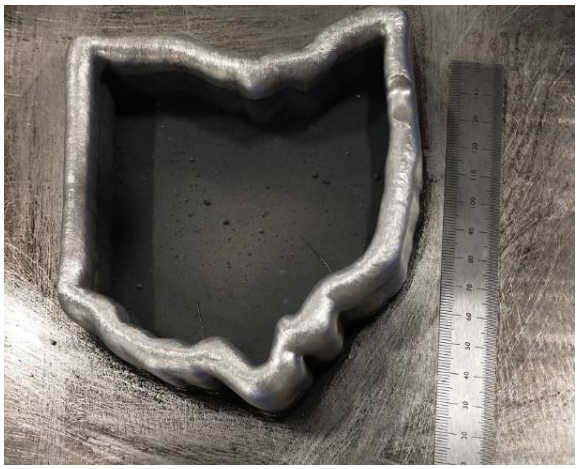

Figure 1: Deposited thin-wall ER5183 State of Ohio outline

Crucial to all applications of DED is the development and refinement of software tools to enable automated robotic toolpath planning and welding process control to produce builds of increasing complexity (11). Further, the scalability and inter-robot compatibility of these robots is of concern as most research and commercial investment in these tools is limited to a single robot cell configuration or manufacturer, limiting their widespread adoption. Autodesk PowerMill Ultimate, formerly known as Delcam, is a mature CAM software platform used widely for traditional subtractive manufacturing operation. PowerMill offers arc DED toolpath generation on its "robot-agnostic" platform. This platform incorporates modelling a digital twin of any robot cell and coding a post-processor to provide the desired arc DED capability. The digital workflow includes modifying CAD geometry for build, "slicing" the digital model for path planning, and

post-processing the robot program for manufacture. Once a digital twin and post-processor is developed for a given robot and cell configuration, it can be freely copied and utilized by any other end-user, reducing the restrictive nature of other proprietary platforms. An example highlighting the use of PowerMill to produce a novel geometry is shown in Figure 1 using an outline of the Ohio state borders.

The bulk of DED research focuses on high cost alloys systems (titanium- and nickel-based) stainless steels, high strength steels, and other welding-based wire consumables. This leads to a gulf of knowledge associated with applying GMA arc DED technology to produce components using aluminum alloys (3, 12). Arc deposition of aluminum alloys requires additional process measures to minimize susceptibility to deposit porosity, lack of fusion and hot cracking. Given the increasing use of aluminum in vehicle and marine applications, development of these capabilities was deemed vital to advance the manufacturing capabilities of arc DED. Al-Mg alloy ER5183 was selected as the wire feedstock for this work as it is used across manufacturing industries, offering the best combination of as-deposited strength, toughness, weldability, and corrosion resistance among aluminum alloy classes. Further, this alloy is non-heat treatable which will be important considering the repeated thermal cycling introduced by the layer by layer melting and re-melting of the process. Additionally, other researchers have had success producing components using this alloy system with a variety of process variations. (1,2,5,7,10)

When considering gas metal arc welding of aluminum, numerous approaches to ensure quality welding have been established. Of the highest importance is the actual welding waveform employed to provide a stable arc and metal transfer with no spatter which leads to consistent metal deposition. Consistency is critical for accurate prediction of bead geometry and digital manufacturing parts using DED processes. GMA DED processes offer a wide range of metal transfer modes. Spray transfer utilizes the highest current among GMA metal transfer modes to provide the greatest deposition rate and highest heat input. Pulsed GMA offers similar deposition rates to standard spray transfer but regularly pulsing current values between a high (peak) and low (background) current value reduces heat input and enables all-position welding capability (6). Cold Metal Transfer (CMT) is another alternative welding technique which employs short circuit transfer with an additional step of wire retraction once transfer is detected to reduce weld current. The advantages to this process come in the form of lower heat input, low spatter, and reduce hydrogen porosity but drawbacks include heightened equipment costs and reduced deposition rate (1,7,9)

Difficulty in arc welding aluminum alloys is owed primarily to its high thermal conductivity, reactivity for forming oxides, and hydrogen solubility. This combination of factors generates a narrow process window. With thermal conductivity an order of magnitude higher than that of steel, discontinuities appear easily when inadequate heat input is applied. Further, the initial layers, close to the heat sink of the build plate, will require increased heat input compared to higher layers. Excessive deposit heat input can lead to loss of predicted geometry and microstructural coarsening. Deposit size heat input needs to be precisely controlled layer by layer until a steady state is reached based on part section thermal conditions. The formation of the tenacious aluminum oxide in air leads to challenges in arc welding as the high melting point of this oxide layer (2072°C compared to 660°C of pure Al) can restrict fusion. Lack of Fusion (LOF) can form between deposit if the pool is not shielded properly with inert gas. Further, the aluminum oxide layer is hydroscopic and readily

absorbs atmospheric moisture. This moisture, if present at any point of the welding process, can lead to gas porosity as solubility of hydrogen increases twenty-fold in liquid aluminum compared to solid. Rapid solidification during welding limits diffusion of supersaturated hydrogen out of the pool and promotes porosity formation as observed by numerous researchers using arc welding with ER518 (1,7,9). Proper cleaning and shielding are essential or excess porosity could cause a reduction in mechanical properties (10). The role of wire feedstock cannot be understated as poor wire surface finish could impact arc stability and disturb the molten weld pool as well as introduce shielding gas contamination (10). Similarly, contaminated wire will serve to directly add unwanted moisture into the molten pool. Storage of wire in dry and sealed conditions is necessary.

The objective of this work was to generate ER5183 GMA-P arc DED builds of increasing complexity containing both single-pass and multi-pass wide wall sections using the developed parameter sets. These feature types were also used to evaluate PowerMill Ultimate's DED tools and support transition of GMA-P DED of ER5183 for structural aluminum component manufacturing.

2. ER5183 GMA-P PARAMETER DEVELOPMENT

Systematic parametric development was used to identify optimal welding parameters for pulsed gas metal arc welding with ER5183 feedstock. A typical deposit size was characterized by producing bead on plate, then walls, and then blocks to progressively establish suitable parameters. This heuristic approach, incorporating many elements of the ARCWISE methodology (13), was used to develop relationships between deposition rate (travel speed) and power on fusion quality using constant deposit area and arc condition tests. For each test, deposit area was controlled by maintaining a constant wire feed speed (WFS) to travel speed (TS) ratio. Deposit and build quality were evaluated using visual and metallographic inspection. The GMA-P DED process used 0.045 in. ER5183 with 100% Ar shielding using an OTC NV6 robot, FD11 robot controller, and Welbee P500L welding power supply. Pulse droplet metal transfer was provided over a large range of wire feed speed using this synergistic power supply on the Pulsed Hard Aluminum preset (13). Contact tip to work distance was held at 5/8" with a torch normal configuration for all welding. The work piece of Al-5083 was clamped to a tilt-turn positioner with care taken to ensure effective grounding. For surface preparation, mechanical removal of the oxide layer on the surface of the baseplate used a ceramic grinding disk or milling bit/disk for the first layer with an acetone wipe before and after. For subsequent layers, a stainless steel wire brush was used to break up any thin oxide layer that formed and remove the vaporized Al/Mg smut that formed on the surface of the part. Inter-pass temperature control at 150°F was used to prevent excessive heat accumulation which could lead to undesirable grain growth and oxide layer formation. If excessive heating was observed, air cooling was used to reduce the hold-time between build deposits. Cooling hold-time was a function of deposition time with 30-60 seconds typical.

It is important to note that across experimentation, microporosity was consistently observed in test metallographic cross-sections. Extended time was spent to isolate potential sources of moisture producing this porosity. Numerous surface preparation approaches were explored to remove the aluminum oxide layer as this is historically the primary source of moisture leading to porosity. Best results were obtained by milling the base plate immediately prior to welding to mechanically remove 1-2mm of material. Smoothing of the aluminum oxide layer into the surface, not removal, was observed when using a grinding disk which led to a relative

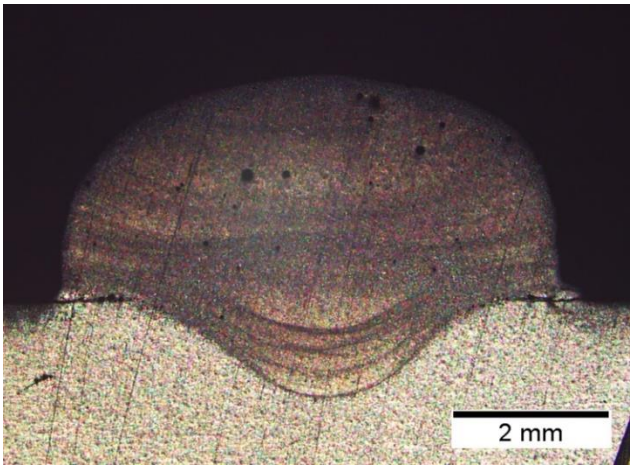

Figure 2: Deposit analyzed with WFS = 350ipm, etched, indicating poor toe fusion and reduced dilution

increase in porosity. Other methods which aimed to modify process conditions, with little effect, include varying push/pull angle, modifying gas flow rate, changing wire liner, drive rolls, wire feedstock (and supplier), or gas bottle, and using linear trail shielding to provide additional shielding. The assumption held is that microporosity is purely a function of experimental setup and work into parametric modeling and arc DED builds will hold validity once setup is further refined.

Bead on plate experiments were the first step to develop of DED parameter sets. Single stringer beads were produced using a ratio of wire feed speed (WFS) divided by travel speed (TS) of 15 at constant arc length of 1/8" over a range of WFS from 300-450 inches per minute and corresponding travel speeds. Constant arc length tests were performed to evaluate the range of deposit quality for this deposit size from lack of fusion to excessive penetration and pool melting. Constant deposit area parameter sets are core to digital manufacturing using PowerMill since the slicer is based on the deposit area. To ensure, constant arc behavior and arc length over the WFS range, the power supply "arc trim value" parameter was determined as a function of wire feed speed. The Arc Trim value manipulates voltage as well as the pulsed current waveform (9,13). Arc trim values to obtain desired 1/8" arc length, across the range of WFS = 300-450 ipm, were obtained by recording the arc and weld pool behavior using a torch-mounted Xiris XVC-1100e camera. The wire diameter was used as a gauge to measure of arc length between the electrode tip and pool surface. For metallographic cross sections, bead on plate tests were cut, polished to 1200-grit, and etched using Barker's etch at 25V for 2 minutes. This etchant configuration was used throughout the remainder of experimentation.

Analysis was conducted on each bead to establish dilution and evaluate the fusion profile, example shown in Figure 2. Further, a plot of dilution versus WFS is shown in Figure 3. Poor toe fusion was observed at low wire feed speeds since the base material melting efficiency was too low to ensure fusion for this deposit size and heat input. By increasing speed more heat is used for melting even though heat input (KJ/mm) is nearly constant over a range of wire feed speeds. Heat input is dependent on deposit size, arc length and arc metal transfer conditions (electrode size, electrode extension and shielding gas). Depending on the build thermal conditions, the wire speed, travel speed, and power need proportionally adjusted to ensure good contact deposit area fusion.

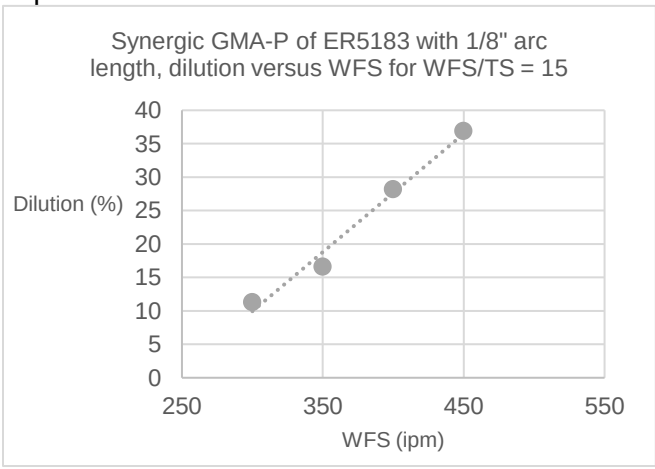

Figure 3: Plot of dilution versus WFS for WFS/TS=15

After bead on plate layer 1 parameters were determined, walls parameters were systematically characterized using the same constant deposit area approach for layer 2 through 5. A waterfall deposit wall test approach, as shown in Figure 4, was used so a remnant of each layer was available for visual examination. For each layer, a range of WFSs and TSs were evaluated to determine preferred parameter sets per layer.

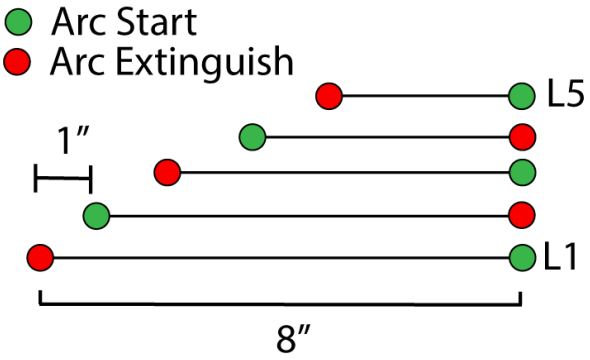

Figure 4: Waterfall build strategy enabling analysis of steady-state region of each layer

The WFS, TS, and power were reduced for each subsequent layer. This was required as the material capacity for heat transfer was reduced by moving further from the build plate. Based on prior trials with different bead sizes, a steady state was obtained typically between layers 3 through 5 so the waterfall tests were limited to 5 layers. Without reductions in deposition parameters with increasing layer height, bead geometry was shown to droop on either side of the previous bead. Too much melting increases molten pool fluidity and promotes loss of wall edge surface fairness. Through experimentation preferred parameters sets reduced wire feed speed in increments of 50 ipm from 450 ipm / layer 1 with steady-state wall welding parameters obtained using WFS = 350 ipm for layer 3 and upward. The regions of arc starting and arc extinguishing, referred to as start/stops, are a source of geometric abnormality and were neglected in this stage as emphasis was placed on the steady-state center region.

Layer height was predicted from the identified bead geometries of single bead trials using a value of 80% the stringer bead reinforcement height. Accurate layer height prediction was important to maintain a constant contact tip to work distance to guarantee consistent deposition profile. If contact tip to work distance varied, unexpected arc behavior led to unpredictable weld geometry. To maximize deposition rate, the highest WFS of the process window was selected before necessary reductions were identified and incorporated.

Visual inspection of walls considered quality of fusion and observation of any visible defects at the surface of beads. Metallographic analysis of wall samples confirmed adequate fusion profile with an example wall shown in Figure 5. Acceptable vertical fairness between beads with convexity of less than 2mm is displayed. Acceptable fairness, measured as the gap between adjacent beads, aimed to obtained a sub 2mm value across future trials.

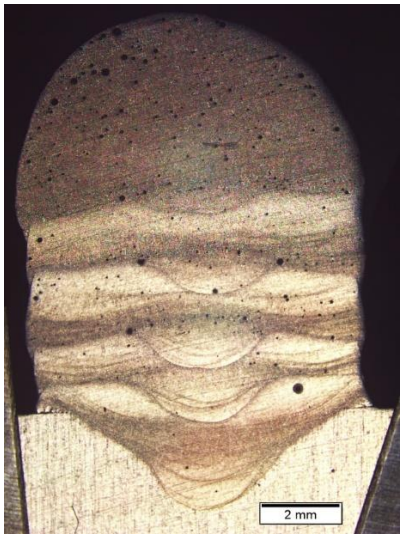

Figure 5: Cross-section of wall build, etched, showing poor toe fusion but good inter-layer fusion and acceptable fairness

Next, “blocks” of 5 beads wide by 5 beads tall were welded to evaluate heat management between deposits and bead overlap distance employing the wall parameters. To balance heating of the part and prevent distortion, deposition followed a staggered strategy with each

layer starting with a center bead and progressing outward laterally, shown in Figure 6.

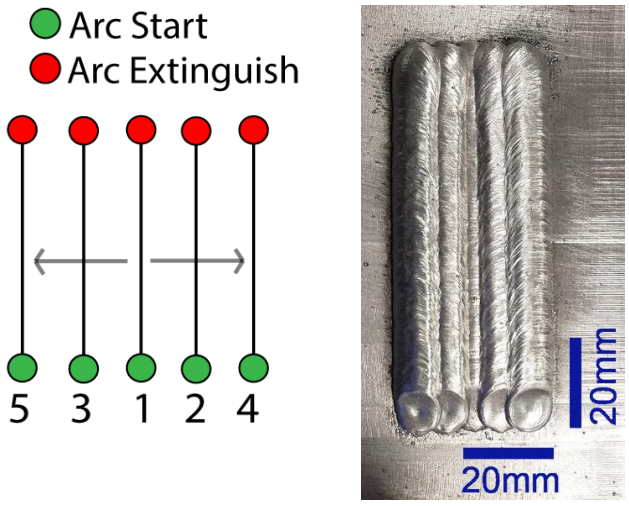

Figure 6: Single layer of block deposition strategy with outward symmetry, displayed in trial

As the center bead experienced much greater heating and remelting during each subsequent deposition, sagging occurred leading to reduced horizontal fairness across layers, inspiring further exploration into modifying center bead parameters. To guarantee a fully sound part, the spacing between each deposited bead is of critical importance. Too large a gap would lead to lack of fusion "voids" and too small would lead to a breakdown in predicted geometry and excessive local reinforcement. In contrast with literature values which suggest an overlap distance of between 60-75% of bead width, an overlap distance of 55% of measured bead width provided the best fusion, surface fairness and no void formations during block builds with ER5183 GMA-P DED. Visual inspection of wall builds evaluated fairness across sidewalls and along the top of the final layer, desired appearance is shown in Figures 7 and 8. Metallographic inspection of the block builds using preferred parameters demonstrated uniform fusion profiles per bead and layer, Figure 9.

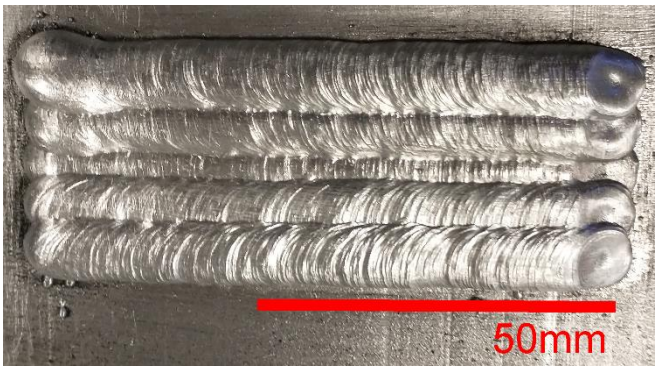

Figure 7: Desirable block visual appearance, overhead view

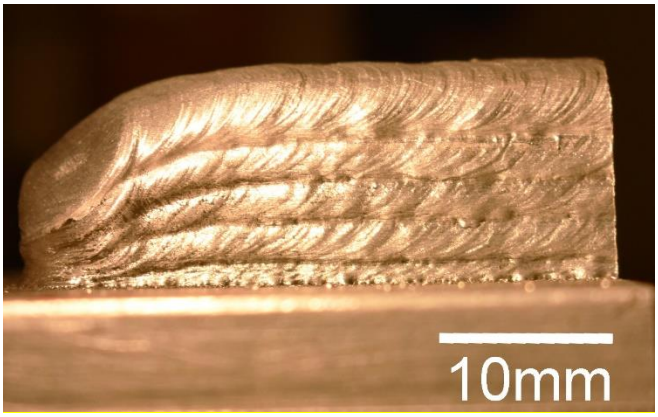

Figure 8: Desirable block visual appearance, side view

A range of discontinuities were also observed when using unacceptable parameters sets and / or conditions. For example, Figure 10 shows an unetched metallographic section that contains un-melted oxide layer inclusions between deposits, An inadequately cleaned stainless steel wire brush for cleaning between each pass was considered a possible explanation for appearance of these unwanted inclusions between deposits as later cleaning of the brush removed the incidence of discontinuities on boundaries. Use of a solvent rinse with ultrasonic cleaning was seen to eliminate contaminants from the wire brush.

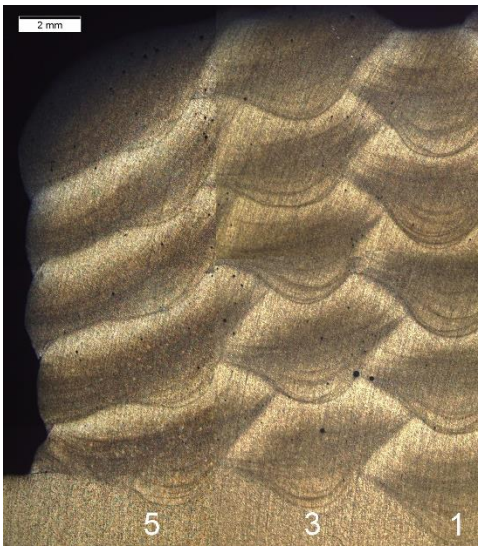

Figure 9: Etched cross-section of block build

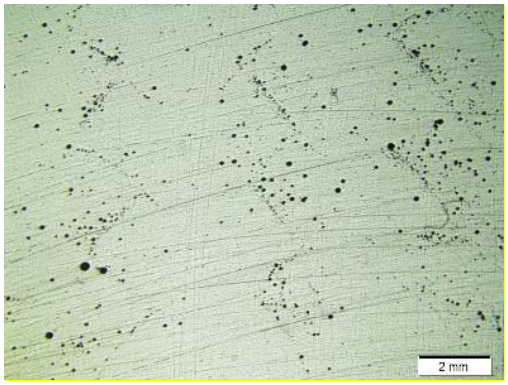

Figure 10: Porosity and inter-layer oxide inclusions between deposits in block build

To address poor fusion profiles at the toe of beads and lack of fusion between beads in blocks, linear oscillation of the torch during welding was examined to improve underbead fusion profile and heat distribution. It is well known that aluminum welding with heavier argon gas shielding may promote lack of fusion at the deposit toes. Argon-helium mixture or helium shielding gas can produce a hotter arc and larger heat field but significantly increase gas costs. For this reason, helium was not considered for this project to drive build economics. To improve bead fusion, the selected robotic torch oscillation parameters were 0.8mm amplitude (oscillation width), 2.5 Hz (oscillation / second) with 0.1 dwell time on each oscillation weave. The same relationships previously established for bead overlap and layer height were employed. Oscillation effectively addressed lack of fusion and poor toe fusion in walls and blocks, as shown in Figures 11 and 12. Using the preferred wall parameters and adding oscillation resulted in a decreased effective travel speed based on the OTC programming method. The use of a 0.1 second dwell reduced travel speed during welding by 30%, breaking from the established WFS/TS ratio but ensuring quality fusion as evidenced by metallographic results. The oscillated wall used a WFS/TS ratio of 25. The geometric modification owed to oscillation can be observed in the shifting of the deposit horizontally throughout deposition, further observed as a reduced vertical fairness value when compared to non-oscillated block builds. Future work will repeat the systematic Arcwise experiments to create preferred parameters for this larger deposit with oscillation.

Figure 11: Block utilizing torch oscillation with improved inter-bead and toe fusion, reduced fairness

Figure 12: Wall utilizing 2.5 Hz torch oscillation, etched, with excellent toe fusion. Vertical fairness needs improvement through additional parameter refinement.

3. UTILIZATION OF POWERMILL ULTIMATE FOR ARC DED

This project evaluated the digital twin and Autodesk PowerMill platform for an OTC-Daihen welding robot and power supply. The virtual recreation of the robot, known as a digital twin, produced courtesy of EWI, is shown in Figure 13. The digital twin was used to fully simulate the welding process and robot toolpath motion then exported using a post-processor software script to allow for transfer onto the OTC robot cell. Within the PowerMill environment, there is a high degree of control over robot motion, toolpath position, and tool orientations, allowing for fine tuning of deposition.

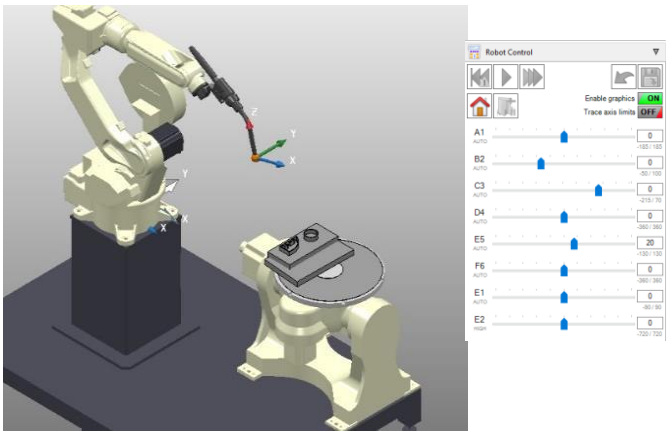

Figure 13: OTC V8 Digital Twin (Courtesy EWI)

Established weld parameter sets were applied directly to produce ER5183 representative builds with full robot and power supply control in PowerMill. Thin-wall builds of 2 walls per layer and thick-wall builds of 8 beads per layer were created with each iteration providing insight into design rules and considerations for quality ER5183 DED builds. Critical aspects of arc DED toolpath management, relying on functionality within PowerMill, include the management of deposition order and configuring arc start/stop locations. Deposition order can significantly impact deposition geometry as the distortion and heat cycling introduced during deposition will cause a shift from expected geometry. Depositing material “inside-out” for thin-wall builds was identified as appropriate to ensure quality fusion. Further, as all deposition was conducted in a torch normal approach, welding the internal most bead first provided improved access for the welding head and will enable future torch and work angle modifications, if needed, for further fusion improvements. Similarly, following the deposition schema employed for block builds, varying deposition order inside out symmetrically enabled viable thick-wall builds. Management of start/stop location aimed prevent defects forming from bead abnormality at the arc start point which could cause consecutive layer height differences, referred to as height error, as the process

continues, eventually reaching an unacceptable point. To address this, start/stop locations of each layer were shifted around the boundary of the part by 30 degrees for each layer around the center of the build. This shifting of start/stop location was vital to maintain expected bead geometry as subsequent beads would eventually smooth out the increased height at that abnormal start/stop region. Alternatively, use of an intentionally detachable start/stop location, commonly done for multi-pass welding, would be a suitable and feasible approach to limit the impact of this abnormality as it would be removed following welding.

Three representative builds utilizing PowerMill Ultimate will be discussed: a thin-wall build of a simple rectangle with rounded edges extruded upward, a thin-wall build of a cone with a slight overhang, and a thick-wall build of a flat region and triangular region using oscillation. All builds were produced employing the findings of parameter development for deposition strategy, bead spacing, and weld parameters.

A 2-bead per layer build of a rounded rectangular shape with an angled upper wall was produced in 51 layers with a ER5183 layer height of 2mm, shown in Figure 14.

Figure 14: Deposited 2.5D thin-wall build

Toolpaths produced in PowerMill, shown in Figure 15, demonstrate the arrangement of start/stop location for the robot. Rounded corners were selected to examine the impact of corners on heat management.

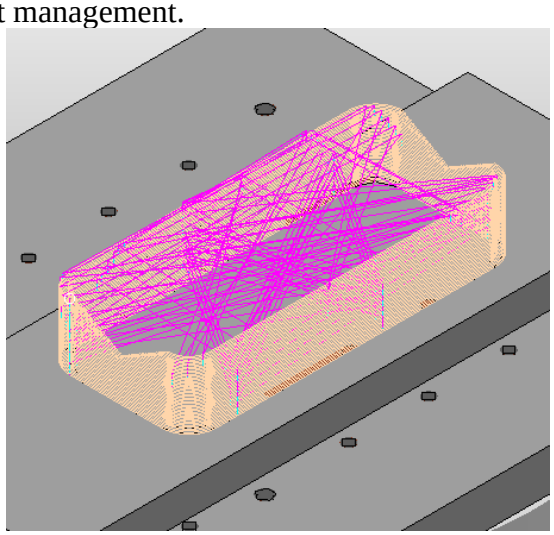

Figure 15: PowerMill-generated robot toolpath visualized

Concentration of heating on the inner or outer bead of corners, depending on deposition ordering, led to subsequent sagging or elevation of the inner/outer radius, as shown in the side view of Figure 16. This side view also provides evidence of good sidewall fusion and desirable fusion profile without too much sagging of beads in the longer steady-state region. Height error emerging at these corners propagated upwards through the build introducing reduced accuracy but did not reach a level that caused failure. This build confirmed the limitations on deposition produced by the selected inter-pass temperature value of 150F as cooling with air required between 60-90 seconds between each deposit to allow for cooling.

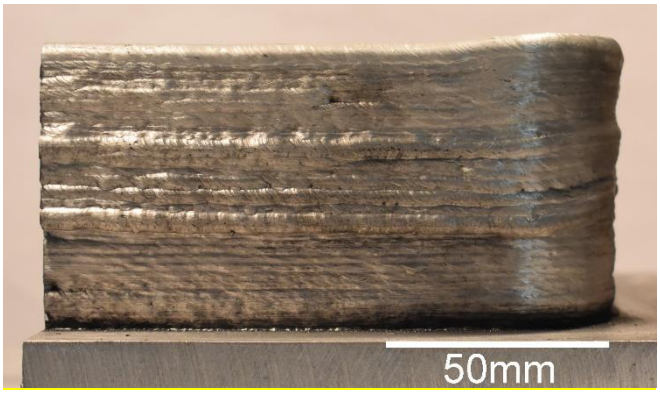

Figure 16: Deposited 2.5D thin-wall build, side view

Metallographic examination of the inner bead and overlap with the outer bead, shown in Figure 17, display inter-deposit oxide inclusions of formed aluminum oxide. Regions of concentrated microporosity are observable on the boundaries of each deposit suggesting contamination on boundaries between layers after deposition. The upper angled wall region employed a single bead for each angled region, demonstrating the impact of increased heating from an adjacent bead causing a loss of predicted geometry for the subsequent bead when no inter-pass temperature control is employed, shown in Figure 18. This geometric inaccuracy contributed to overall height error as it was propagated upward and lead to visible de-coupling and poor fusion between the two beads with visible center gaps. Improving weld tie-in using oscillation to increase toe fusion between beads or employing PowerMill to modify bead overlap distance on higher layer are proposed to address this issue.

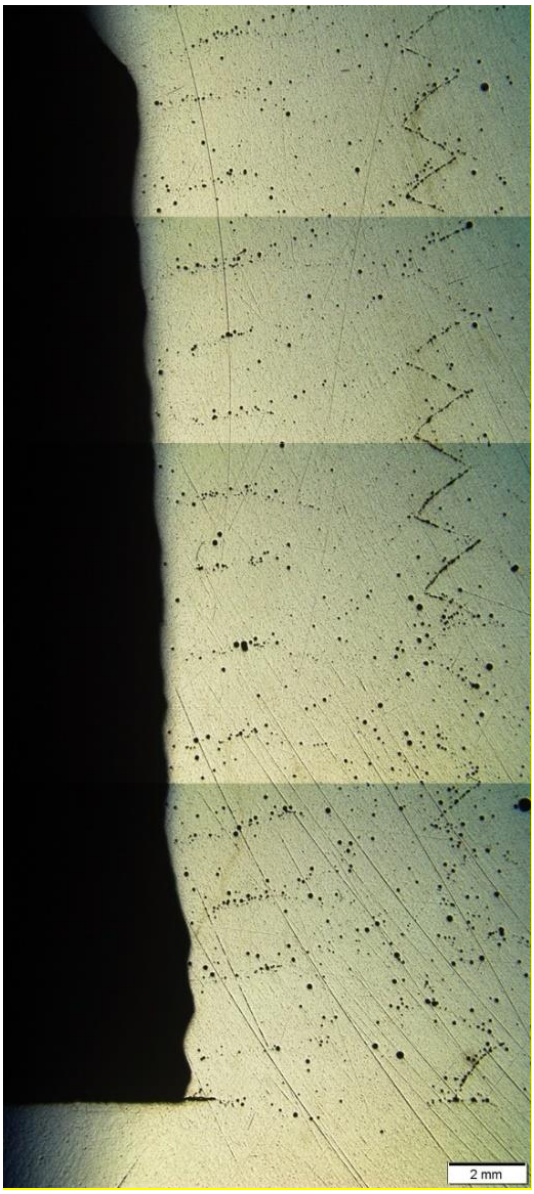

Figure 17: Macro-section of lower region of 2.5D thin-wall build demonstrating LoF and interlayer inclusions

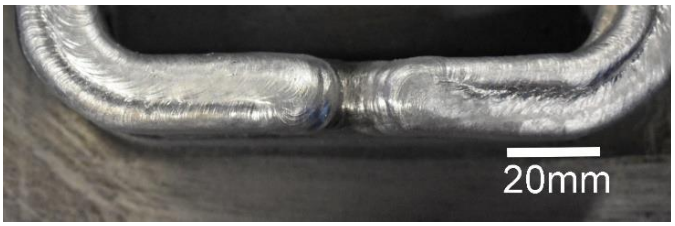

Figure 18: Inner and outer bead sagging, top view

Figure 19: Deposited thin-wall circular build, side view

A 2-bead per layer cone with an overhang of 70° was produced in 35 layers with base diameter of 100mm and top diameter of 150mm using 2mm layer height, shown in Figures 19 and 20. This build featured significant departure from expected geometry very early on into deposition with the inner and outer beads de-coupling during deposition, shown in Figure 21. This contrast of inner and outer bead geometries emerged from the challenge of torch normal deposition with an overhang as the base of the previous layer was inadequate for flat deposition, leading to the sagging of outer beads. Metallography results, shown in Figure 22, highlights similar concerns with voids between the inner and outer beads visible. This large lack of fusion was similarly observed in block builds with an improperly large overlap distance. Rotation of start/stop location effectively limited the incidence of height error stemming from the abnormality of start/stop bead geometry as well. Subsequent layers deposit over this start/stop region and restored uniform layer height. Higher axis future builds will employ a torch work angle for outer beads to improve bead overlap fusion as this technique is typical of making fillet weld deposits. A work angle will concentrate more heat into the weld toe of the prior deposit ensuring better fusion and build fairness.

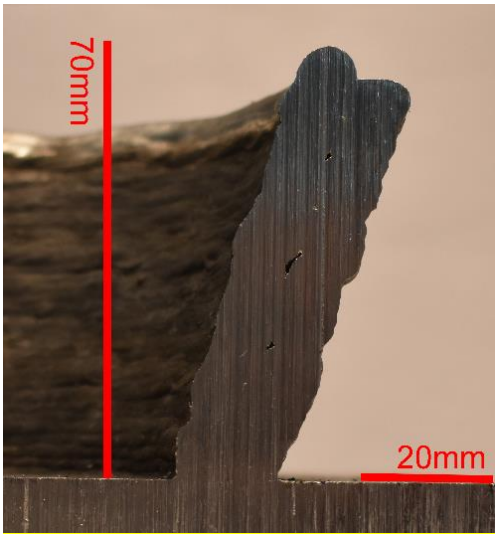

Figure 20: Deposited thin-wall circular build, sectioned side view

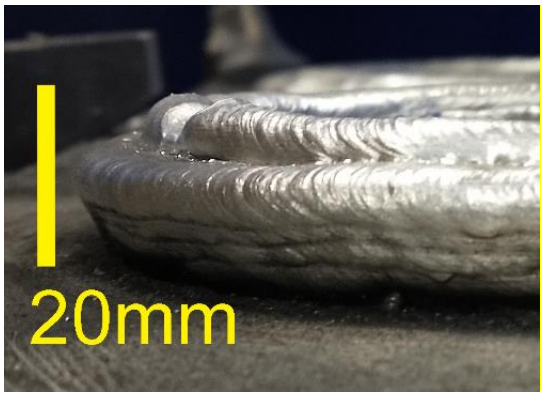

Figure 21: Deposited thin-wall circular build, de-coupling of bead

Figure 22: Macrosection of thin-wall circular build, inter-bead void and inter-layer porosity visible

An 8-bead per layer base triangular section build was produced in 18 layers using PowerMill control with torch oscillation and a 2.4mm layer height, shown in Figure 22 and 23. Start/stop control was not directly employed as emphasis was on the fusion quality and increased deposition rate supported by torch oscillation during deposition. Metallographic results, shown in Figure 24, suggest improvements to fusion quality with no inter-bead discontinuities. The sloping upper region of the block examined the role of previous bead location on future bead deposition with adequate fusion demonstrated throughout. This build suggests and supports broad incorporation of torch oscillation to improve deposition rate and reduce the incidence of lack of fusion defects for future ER5183 GMA-P DED.

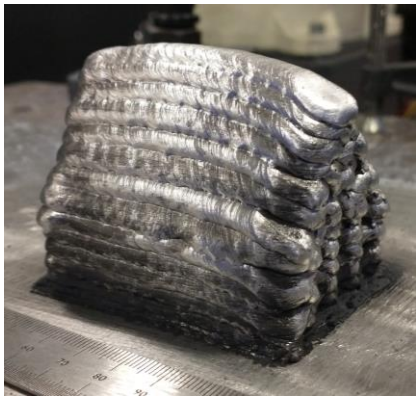

Figure 22: Deposited thick-wall build, orthographic view

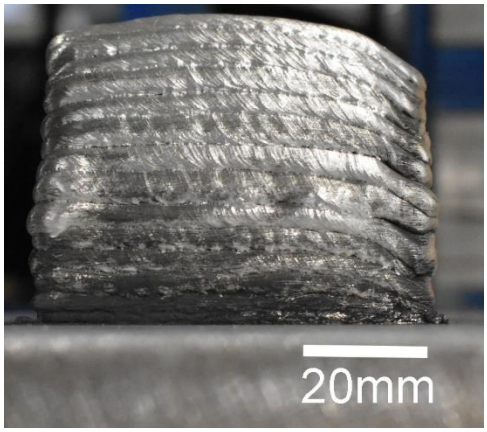

Figure 23: Deposited thick-wall build, side view

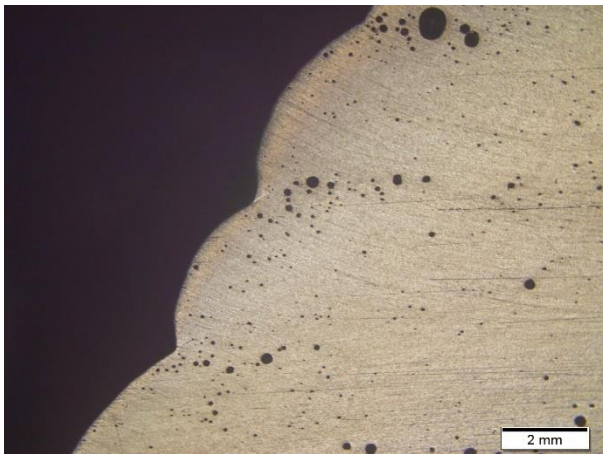

Figure 24: Macrosection of thick-wall sloped edge showing complete fusion and suitable fairness with some porosity.

4. Future Work

Further PowerMill capability emerges through the control of the tilt-turn positioner to which the build plate is clamped. Modifying the orientation of the entire part on the build plate through higher axis control will allow torch work angle modification and more effective welding deposit positions to be obtained to allow for a variety of feature types. This coordinated motion of robot and positioner, readily available in PowerMill, will introduce complexity to the process and through manipulation of gravity, allow for the printing of overhangs and non-gravity aligned geometry previously not possible. Future work will aim to apply this capability alongside the established model and oscillation parameters to generate larger and more geometrically complex components. Further, numerous toolpath strategies for layer by layer deposition have been demonstrated with the primary two approaches being raster and offset. PowerMill offers both approaches for automated toolpath deposition in addition to the ability to merge multiple strategies of a given layer to achieve improved deposition. Employing a “frame-and-fill” approach uses a raster deposition to fill the internal structure and an offset at the outer perimeter of the component. The demonstrated builds have used only one of the

two available strategies with future work seeking to deploy both in unison to provide greater control and deposition capability.

Qualification features will be identified and produced using ER5183 for tensile properties and transverse Vickers hardness mapping. Greater exploration of process control mechanisms and welding waveform should be employed to produce sound and porosity-free weld deposits of ER5183 for arc DED.

5. Conclusions

1. Arc DED of ER5183 was successfully demonstrated using an OTC GMA-P system with Autodesk PowerMill Ultimate CAM software using preferred parameter sets for common features.
2. A systematic methodology for sound GMA-P parameter development was demonstrated for a range of build features.
3. Suitable wall and block parameters for ER5183 deposits required 10% reduction in power per layer as the build progresses from the build plate until steady-state is obtained at layer 3 upwards.
4. Slicing parameters for multi-bead per layer deposits of ER5183 GMA-P were experimentally determined to be bead overlap of 55% bead width and layer height of 80% bead height.
5. Torch oscillation during GMA-P of ER5183 improved inter-bead, inter-layer, and toe fusion by improving heat distribution and resultant underbead shape. Further work is needed to build parameter sets that incorporate oscillation and torch work angle based on advanced feature requirements.
6. Aluminum oxide inclusions and high hydrogen solubility necessitate greater process control for porosity-free deposition and guarantee mechanical properties.

6. REFERENCES

[1]
A. Horgar, H. Fostervoll, B. Nyhus, X. Ren, M. Eriksson, and O. M. Akselsen, “Additive manufacturing using WAAM with AA5183 wire,” *Journal of Materials Processing Technology*, vol. 259, pp. 68–74, Sep. 2018, doi: 10.1016/j.jmatprotec.2018.04.014.

[2]
X. Fang *et al.*, “Correlations between Microstructure Characteristics and Mechanical Properties in 5183 Aluminium Alloy Fabricated by Wire-Arc Additive Manufacturing with Different Arc Modes,” *Materials*, vol. 11, no. 11, p. 2075, Oct. 2018, doi: 10.3390/ma11112075.

[3]
T. A. Rodrigues, V. Duarte, R. M. Miranda, T. G. Santos, and J. P. Oliveira, “Current Status and Perspectives on Wire and Arc Additive Manufacturing (WAAM),” *Materials*, vol. 12, no. 7, p. 1121, Apr. 2019, doi: 10.3390/ma12071121.

[4]
“F3187 Standard Guide for Directed Energy Deposition of Metals.” ASTM, 2016.

[5]
J. Xiong, Y. Lei, H. Chen, and G. Zhang, “Fabrication of inclined thin-walled parts in multi-layer single-pass GMAW-based additive manufacturing with flat position deposition,” *Journal of Materials Processing Technology*, vol. 240, pp. 397–403, Feb. 2017, doi: 10.1016/j.jmatprotec.2016.10.019.

[6]
A. Joseph, D. Farson, D. Harwig, and R. Richardson, “Influence of GMAW-P current waveforms on heat input and weld bead shape,” *Science and Technology of Welding and Joining*,

vol. 10, no. 3, pp. 311–318, Jun. 2005, doi: 10.1179/174329305X40624.

[7]
B. Zhang, C. Wang, Z. Wang, L. Zhang, and Q. Gao, "Microstructure and properties of Al alloy ER5183 deposited by variable polarity cold metal transfer," *Journal of Materials Processing Technology*, vol. 267, pp. 167–176, May 2019, doi: 10.1016/j.jmatprotec.2018.12.011.

[8]
J. P. Oliveira, T. G. Santos, and R. M. Miranda, "Revisiting fundamental welding concepts to improve additive manufacturing: From theory to practice," *Progress in Materials Science*, vol. 107, p. 100590, Jan. 2020, doi: 10.1016/j.pmatsci.2019.100590.

[9]
J. Gu, J. Ding, S. W. Williams, H. Gu, P. Ma, and Y. Zhai, "The effect of inter-layer cold working and post-deposition heat treatment on porosity in additively manufactured aluminum alloys," *Journal of Materials Processing Technology*, vol. 230, pp. 26–34, Apr. 2016, doi: 10.1016/j.jmatprotec.2015.11.006.

[10]
E. M. Ryan, T. J. Sabin, J. F. Watts, and M. J. Whiting, "The influence of build parameters and wire batch on porosity of wire and arc additive manufactured aluminium alloy 2319," *Journal of Materials Processing Technology*, vol. 262, pp. 577–584, Dec. 2018, doi: 10.1016/j.jmatprotec.2018.07.030.

[11]
D. Ding *et al.*, "Towards an automated robotic arc-welding-based additive manufacturing system from CAD to finished part," *Computer-Aided Design*, vol. 73, pp. 66–75, Apr. 2016, doi: 10.1016/j.cad.2015.12.003.

[12]
D. Jafari, T. H. J. Vaneker, and I. Gibson, "Wire and arc additive manufacturing: Opportunities and challenges to control the quality and accuracy of manufactured parts," *Materials & Design*, vol. 202, p. 109471, Apr. 2021, doi: 10.1016/j.matdes.2021.109471.

[13]
D. Harwig, "Wise Method for Assessing Arc Performance," *Welding Journal*, pp. 35–39, Dec. 2000.